HAL
open science

Functional fluorescent organic nanoparticles

Elisa Campioli

To cite this version:

Elisa Campioli. Functional fluorescent organic nanoparticles. Other. Université de Rennes; Università degli studi (Parme, Italie), 2013. English. NNT : 2013REN1S009 . tel-00954407

HAL Id: tel-00954407

https://theses.hal.science/tel-00954407v1

Submitted on 14 May 2014

HAL is a multi-disciplinary open access archive for the deposit and dissemination of scientific research documents, whether they are published or not. The documents may come from teaching and research institutions in France or abroad, or from public or private research centers.

L'archive ouverte pluridisciplinaire **HAL**, est destinée au dépôt et à la diffusion de documents scientifiques de niveau recherche, publiés ou non, émanant des établissements d'enseignement et de recherche français ou étrangers, des laboratoires publics ou privés.

ANNÉE 2013

THÈSE / UNIVERSITÉ DE RENNES 1
sous le sceau de l'Université Européenne de Bretagne

En Cotutelle Internationale avec
Università degli Studi di Parma

pour le grade de

DOCTEUR DE L'UNIVERSITÉ DE RENNES 1

Mention : Chimie

Ecole doctorale Sciences de la Matière

présentée par

Campioli Elisa

préparée à l'unité de recherche UMR 6510 CNRS/UR1
Chimie et Photonique Moléculaire

Functional Fluorescent Organic Nanoparticles

Thèse soutenue à Parma le 01/03/2013

devant le jury composé de :

Suzanne FERY-FORGUES
Institut des Technologies Avancées en sciences du Vivant (ITAV)
rapporteur

Olivier MONGIN
Sciences et Propriétés de la Matière
Institut des sciences chimiques de Rennes1
examinateur

Michele SUMAN
Barilla SpA, Food Research Labs
Via Mantova 166, 43122 Parma (Italy)
examinateur

Franco UGOZZOLI
Università degli Studi di Parma
Dipartimento di Chimica
examinateur

Contents

List of Abbreviations **v**

Introduction **1**

1 Organic Nanoparticles: Preparation and Characterization **5**

1.1 Preparative Methods 5

1.1.1 Hydrosols Systems from Hydrophilic Solvents 7

1.1.2 Hydrosols Systems from Lipophilic Solvents 8

1.2 Theoretical Approaches 10

1.2.1 Classical Nucleation Theory 10

1.2.1.1 Homogenous Nucleation: Thermodynamic Aspects 10

1.2.1.2 Homogenous Nucleation: Kinetic Aspects . . 13

1.2.1.3 Mechanism of Growth 15

1.2.2 Aggregation 16

1.3 Characterization Methods 19

1.3.1 Optoelectronic Properties 19

1.3.2 Morphological Properties 20

1.3.2.1 Microscopy Methods 20

1.3.2.2 Dynamic Light Scattering 21

1.4 Experimental 23

1.4.1 Triphenylamine-based derivatives 24

1.4.1.1 T1 and T2 Nanoparticle Suspensions 25
1.4.1.2 T3 and T4 Nanoparticle Suspensions 32
1.4.2 Thiophene-based derivatives 35
1.4.2.1 TP1 and TP2 Nanoparticle Suspensions . . 36
1.4.3 Bodipy derivatives 39
1.4.3.1 MB Nanoparticle Suspension 40
1.4.4 Commercial Chromophores: Nilered and DCM 44
1.4.4.1 Nilered and DCM Suspensions 44
1.5 Conclusions 47

2 Fluorescent Organic Nanoparticles as Biphotonic Probes 49
2.1 Two-Photon Microscopy 49
2.1.1 *In Vivo* Imaging 52
2.2 Biphotonic Probes 54
2.2.1 Quantum Dots 55
2.2.2 Dye-loaded Silica Nanoparticles 57
2.2.3 Fully-Organic Probes 57
2.2.3.1 Nanodots 58
2.2.3.2 Organic Nanoparticles 61
2.3 Two-Photon Excitation Fluorescence of Triphenylamine-based Organic Nanoparticles 62
2.4 *In vivo* Two-Photon Microscopy using Organic Nanoparticles as Probes 68
2.5 Conclusions 71

3 Colloidal Stabilization of Organic Nanoparticles 73
3.1 Classical Methods for Stabilizing Colloids: Overview 73
3.1.1 Electrostatic Stabilization 75
3.1.2 Steric and Depletion Stabilization 76
3.2 Stabilization of Organic Nanoparticles using Ultrasounds and Low-Concentration Additives 77

3.2.1 Preparation of Nanoparticles with Ultrasounds and Additives . . . 78
3.2.2 Morphological Characterization . . . 80
3.2.3 Spectroscopic Characterization . . . 86
3.3 Stabilization of Organic Nanoparticles by "Molecular Design" . . . 94
3.3.1 Synthesis of Chromophores . . . 95
3.3.2 Spectroscopic Characterization . . . 96
3.4 Conclusions . . . 100

4 Organic Nanoassemblies for Energy and Electron Transfer 103
4.1 Introduction . . . 103
4.1.1 Excitation Energy Transfer . . . 104
4.1.2 Photoinduced Electron Transfer . . . 110
4.2 Organic Nanoassemblies for Excitation Energy Transfer . . . 111
4.2.1 Doped Binary Nanostructures . . . 112
4.2.1.1 Preparation of Doped Nanoparticles: "one step" Process . . . 113
4.2.1.2 TW3-doped TW1 nanoparticles . . . 114
4.2.1.3 Nilered-doped T1 Nanoparticles . . . 116
4.2.1.4 T4-Doped T5 Nanoparticles . . . 118
4.2.2 Core@Shell Binary-Nanostructures . . . 121
4.2.2.1 Preparation of Core@Shell Nanoparticles: "multi step" Process . . . 122
4.2.2.2 TW3@TW1 Core@Shell Nanoparticles . . . 122
4.2.2.3 Nilered@T1 Core@Shell Nanoparticles. . . . 134
4.2.2.4 T4@T5 Core@Shell Nanoparticles. . . . 136
4.2.3 Multi Shell Nanostructures . . . 140
4.3 Organic Nanoassemblies for Electron Transfer . . . 155
4.3.1 Preparation of TW3@DiMe-PTCDI Nanoparticles . . 158

4.3.2 Spectroscopic Characterization of TW3@DiMe-PTCDI Nanoparticles 158
4.4 Conclusions 163

Conclusions and Perspectives **165**

Appendix 1 **169**

Appendix 2 **173**

Appendix 3 **175**

Acknowledgments **177**

Bibliography **178**

List of Publications **193**

List of Abbreviations

ACQ *Aggregation-Induced Quenching*
AFM *Atomic Force Microscopy*
AIE *Aggregation-Induced Emission*
CT *Charge Transfer*
DFT *Density Functional Theory*
DLS *Dynamic Light Scattering*
DMSO *Dimethylsulfoxide*
EET *Excitation Energy Transfer*
FONs *Fluorescent Organic Nanoparticles*
NIR *Near Infrared*
NPs *Nanoparticles*
PET *Photoinduced Electron Transfer*
PMMA *Polymethylmethacrylate*
QDs *Quantum Dots*
SEM *Scanning Electron Microscopy*
TEM *Transmission Electron Microscopy*
THF *Tetrahydrofuran*
TPA *Two-Photon Absorption*
TPEF *Two-Photon Excitation Fluorescence*
VDWL *Van der Waals-London*

Introduction

During the past two decades, increasing research attention has been devoted to nanomaterials (materials in the range of 10-100 nm) because of their unique properties. Generally, nanostructures can be divided into inorganic materials, organic macromolecular materials, organic low-molecular-weight nanoparticles and hybrid inorganic-organic nanocomposites.

Zero-dimensional (0D) inorganic nanostructures as nanoparticles, clusters and quantum dots have been well investigated during the last years. For example, works on preparation [1], shape control [2] and size-dependent optoelectronic properties [3] of various nanodevices based on semiconductor quantum dots have been reported by many research groups (such as light-emitting diodes [4], solar cells [5], chemical sensors [6]). Another important area of 0D inorganic nanomaterials is metal [7] and magnetic compound nanoparticles [8] for bio-applications.

Besides inorganic nanomaterials, those composed of macromolecules, such as polymers, biomolecules, dendrimers, ecc., have also been extensively investigated during the past decade. For example, nanospheres have been obtained from polystyrene [9], conjugated polymers [10] or block copolymers [11] by self-assembly and microemulsion processes in solution.

Instead, nanomaterials based on small organic molecules are subject of research only since very recent years, as attested by the few review works on the preparation methods and applications of this type of nanostructures [12, 13]. The reason is twofold: first, these nanomaterials are characterized

by poor thermal instability and mechanical properties that give few routes for nanostructure preparation; second, the optical and electronic properties of the obtained nanoparticles are very difficult to be predicted from the molecular structure. Indeed, differently to what happens in inorganic nanoparticles, weak intermolecular interactions, such as hydrogen bonds, π-π stacking, and Van der Waals contacts, are responsible for the optical and electronic properties of organic nanostructures.

The preparation of organic nanoparticles can be attained principally by two routes:

- the mechanical milling of the raw materials by ultrasounds and/or laser ablation;
- the conversion of the products or educts dissolved in suitable solvents into nanodispersed systems by reprecipitation, condensation or by specific procedures.

At the moment little is know about the molecular processes which take place during the mixing of two starting solutions for producing the state of supersaturation which initiates particles formation. Understanding the mechanism of organic nanoparticles formation is of prime importance because it can lead, by variation of process parameters, to a specific manipulation of final properties, as size, shape, stability, optical behavior, ecc.

However, organic nanomaterials have gained more and more attention for their unique optoelectronic properties such as size-dependent optical properties [14], luminescence [15], large nonlinear optical efficiency [16, 33]; they are thus expected to serve as novel functional materials in electronics and photonics.

Another very recent class of organic nanostructures consists of so-called organic nanocomposites, obtained by two or more different starting compounds. They differ from hybrid inorganic-organic materials because they

are composed only of organic compounds; an example of this new class of nanostructures are doped organic nanoparticles, that show very interesting properties, such as tunable emissions [19].

In this thesis the attention is focused on the preparation and characterization of organic nanoparticles and nanocomposites derived from different types of small organic molecules, their stabilization and the use of these materials as biphotonic probes for bio-imaging [17]. Furthermore, new types of organic binary and ternary nanoassemblies for biologic and optoelectronic applications with unique optical properties have been developed [18].

In Chapter 1 we describe some methods used to obtain this type of nanoparticles focusing the attention on the description of the reprecipitation process and the classical nucleation theory. In the experimental section, we focus the attention on the spectroscopic characterization of fluorescent organic nanoparticle (FONs) suspensions, their colloidal stability during time and the morphological characterization of the obtained nanostructures. We also demonstrate that not all the starting chromophores are adequate to lead stable suspensions.

In Chapter 2 we briefly describe the multiphoton microscopy technique and the most popular inorganic and organic (or hybrid organic/inorganic) biphotonic probes such as quantum dots, dye-loaded silica nanoparticles and nanodots. Then, we focus the attention on the use of fluorescent organic nanoparticles as biphotonic probes and we report a study on FONs designed for this purpose. Those nanostructures have been fully characterized from a spectroscopic and morphological point of view and finally tested for *in vivo* multiphoton microscopy.

Chapter 3 is dedicated to the strategies for stabilizing colloidal nanoparticle suspensions. In the first part of the chapter the most popular strategies of stabilization are described, such as electrostatic, steric and depletion stabilization processes. In the second part we describe two alternative methods to improve the colloidal stability: the use of different types of additives dur-

ing the preparation process, and the molecular design. This last method can be briefly described as conceiving organic dyes whose molecular structure is intended to favor stable colloidal suspensions during time.

The last part of this thesis, Chapter 4, is focused on novel types of organic nanoassemblies conceived to obtain efficient energy and electron transfer between the chromophores that compose the same nanostructure. In the first part of the chapter we describe energy and electron transfer processes from a theoretical point of view, while in the second part we describe the experimental results. In particular, the preparation and the spectroscopic and morphological characterization of fully organic composite and core@shell nanostructures in water are reported. Our novel organic binary core@shell nanostructures show unique photo-luminescence properties related to the very efficient energy transfer process that takes place between the two compounds. These novel materials can be seen as a promising green and biocompatible alternative to the inorganic quantum dots in biological applications. We also report the preparation of ternary core@shell@shell nanoassemblies able to provide energy transfer cascade between the three compounds, and the improvement of their photo-luminescence during time by the use of a commercial polymer. In the last part of the chapter we describe the preparation and some preliminary experimental results of a core@shell nanostructure designed for electron transfer. The properties of this last type of nanosystem are actually under study.

Chapter 1

Organic Nanoparticles: Preparation and Characterization

This chapter is basically divided into three parts: in the first part the reprecipitation methods for the preparation of organic nanoparticles and the classical nucleation theory are described; in the second part the characterization methods for the detection of optoelectronic and morphological characteristics of nanostructures are briefly summarized; the last part focuses on the experimental results on some fluorescent organic nanosuspensions obtained from different organic chromophores.

1.1 Preparative Methods

Organic nanoparticles are nanoaggregates entirely composed by organic molecules (or polymers); their dimension is typical of nano-objects, with diameter in the range of 10 - 100 nm.

Nanodispersed organic systems can be generally obtained in two ways:

- by mechanical milling of bulk materials (ultrasounds or laser ablation);

- by precipitation or condensation of the products or educts.

In both techniques, additives such as surfactants and polymers can be added as colloidal stabilizers.

The use of ultrasounds in milling processes is, in principle, unsuitable for the production of systems with a narrow size distribution because this technique favors the aggregation of smaller particles [12]. Instead, with the use of laser ablation, concentrated nanoparticle dispersions have recently been obtained [20, 21, 22]. In this method microcrystals are suspended in water (or another solvent in which molecules are not soluble) and exposed to intense laser pulse that induce the fragmentation of the microcrystals.

An overview of the production of organic nanoparticles in aqueous media by precipitation and condensation methods is reported in Figure 1.1. Starting from a hydrophobic organic compound, three types of processes can be differentiated depending on the type of solvent [12]:

1. **Lipophilic solvent** (I and II). In this case nanoparticle formation takes place in o/w microemulsion, thanks to the evaporation of the lipophilic solvent that promotes the conversion of the emulsion into a nanodispersion.

2. **Hydrophilic solvent** (IV and V). In this process the particle formation occurs by precipitation because of high level of supersaturation obtained by mixing the organic hydrophilic solvent and water.

3. **Amphiphilic solvent** (III). With the use of this type of solvent, nanoparticle formation takes place through a transient emulsion phase that evolves towards a nanodispersed state.

Aqueous nanoparticle dispersions from polymers are also called pseudolatex, while those obtained from small organic molecules are also called hydrosols,

as reported in Figure 1.1. In this thesis the attention is focused on the process that allows to obtain hydrosols (I and V), as described below in detail.

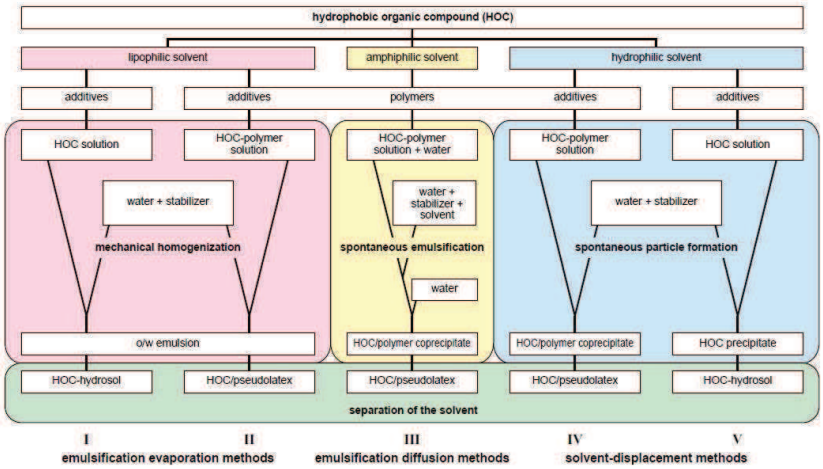

Figure 1.1: Precipitation and condensation processes for the preparation of organic nanoparticles [12].

1.1.1 Hydrosols Systems from Hydrophilic Solvents

The precipitation method to obtain organic nanoparticles was first reported by Nakanishi and coworkers in 1992 [23, 24]. It involves a solvent-exchange process: a concentrated solution of a hydrophobic compound, dissolved in an organic hydrophilic solvent, is rapidly introduced into a large amount of water under vigorous stirring. The rapid mixing of the stock solution with the poor solvent changes the micro-environment of the molecules and induces the precipitation of the compound, which generally forms micro/nanoaggregates or micro/nanocrystals. Hydrophilic solvents used for setting the highest supersaturation possible can be small-chain alcohols, acetone, acetonitrile or tetrahydrofuran (THF). In detail, the following conditions must be fulfilled:

- Nucleation must take place at the highest level of supersaturation possible to maximize the nucleation rate.
- The limitation of particle growth and the setting of a narrow size distribution require a controlled and rapid reduction in supersaturation subsequent to the nucleation step. This can be achieved using sufficiently low active-compound concentration so that secondary crystallization or particle agglomeration processes can be limited. The use of additives as specific growth inhibitors can also be considered.

With the reprecipitation method, a series of organic nanoparticles were successfully prepared by several groups. For example, Nakanishi's, Majima's and Barbara's groups prepared and studied perylene nanoparticles [25, 26], Horn and coworkers prepared nanoparticles from β-carotene [27] and Yao's and Park's groups studied the size dependence of the luminescence and the enhanced emission of nanoparticles prepared in this way [28, 29].

The reprecipitation can be monitored by UV-Vis absorption spectroscopy, recording spectra at different time delays after the initial mixing. When any change in the spectrum is no more detectable, the reprecipitation process can be considered as come to an end. Depending on the properties of the molecule, some hours or few seconds are required (Figure 1.2).

1.1.2 Hydrosols Systems from Lipophilic Solvents

The preparation of the nanoparticles can be carried out by dissolving the active compound together with an emulsifier in a suitable lipophilic solvent, then emulsifying this solution with an aqueous solution and finally removing the organic solvent by distillation. The actual precipitation/crystallization takes place in the emulsion droplets during distillation, when the solubility limit is crossed. The final size of the particles depends on the size of the emulsion droplets and the concentration of the active compound. The particle morphology is usually polycrystalline since the solid formation takes

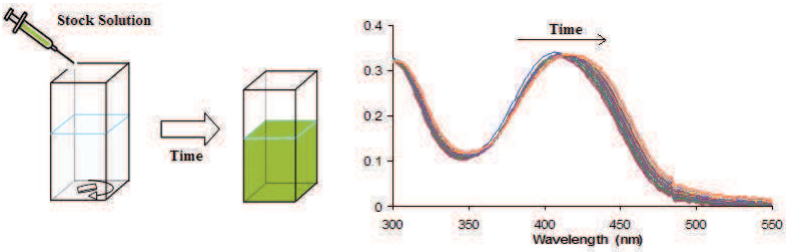

Figure 1.2: In the precipitation method an amount of a stock solution of the small organic compound in an organic hydrophilic solvent is added to a large volume of water under vigorous stirring (left). The process can be monitored by UV-Vis absorption spectroscopy (right).

place by evaporation at low supersaturation. An inherent difficulty in this process lies in the removal of as much solvent as possible from the final product [12]

1.2 Theoretical Approaches

1.2.1 Classical Nucleation Theory

Despite a century of investigations, the nucleation process is still not completely understood. This is particularly true for nanoparticle systems in which nucleation is typically rapid and can be strongly coupled to both growth and Ostwald ripening. One of the most widely accepted models for colloid nucleation is the classical homogenous equilibrium nucleation theory [30].

1.2.1.1 Homogenous Nucleation: Thermodynamic Aspects

For the formation of nanoparticles by homogenous nucleation, a supersaturation of growth species must be created in liquid solution: when the concentration of the solute in a solvent exceeds the solubility limit a new phase appears.

The thermodynamic drive force (or supersaturation) for phase transformation is given by the difference between the chemical potentials of the two individual phases forming the phase boundary. For a liquid-solid system this is given by:

$$\Delta\mu_v = \mu_{solid} - \mu_{liquid} \tag{1.1}$$

where μ_{solid} and μ_{liquid} are the chemical potentials of the liquid and solid phases, respectively. Assuming that in diluted solutions activity approximates molarity and assuming solid incompressibility, the chemical potentials of a bulk species (radius $\rightarrow \infty$) are given by:

$$\mu_{liquid} \approx \mu_e + RT \ln\left(\frac{C}{C^0_{flat}}\right) \tag{1.2}$$

$$\mu^{flat}_{solid} \approx \mu_e \tag{1.3}$$

where R is the gas constant in units $JK^{-1}mol^{-1}$, T is the temperature (K),

$\mu_e$is the equilibrium chemical potential (J/mol), C (mol/m^3) is the real concentration and C^0_{flat} is the equilibrium concentration for a surface with infinite curvature. The supersaturation can therefore be expressed as

$$\Delta\mu_v^{flat} = -RT \ln\left(\frac{C}{C^0_{flat}}\right) = -RT \ln S \tag{1.4}$$

where $S = C/C^0_{flat}$ is typically termed the supersaturation ratio. For systems where the solid phase crystallizes with a finite size (i.e. for nanoparticles), one has to account for the increase of the chemical potential of the solid caused by the significant surface free energy contribution. For spherical particles this factor is described by the Kelvin equation:

$$\mu_s(r) = \mu^{flat}_{solid} + \frac{2\gamma V_m}{r} \tag{1.5}$$

where γ is the surface tension (Jm^{-2}) and V_m is the molar volume (m^3/mol). By combining equations 1.1, 1.2 and 1.5 an expression for the size-dependent chemical potential change for the nucleation of a spherical particle is obtained:

$$\Delta\mu_v(r) = \Delta\mu_v^{flat} + \frac{2\gamma V_m}{r} \tag{1.6}$$

If thermodynamic equilibrium, $\Delta\mu_v(r) = 0$, is assumed, by combining equations 1.4 and 1.6, the Gibbs-Thomson equation is attained:

$$C(r) = C^0_{flat} \exp\left(\frac{2\gamma V_m}{RTr}\right) \tag{1.7}$$

In essence, this relation describes the equilibrium concentration of monomer needed in solution to sustain a particle of radius r. This relationship is at the heart of all nucleation phenomena and has been invoked in practically every growth model of colloids. Its main limitation lies in the questionable definition of surface energy for nanometer sized particles.

The classical nucleation theory assumes that nuclei must overcome a

potential energy barrier due to the newly forming surface area in order to reach a metastable particle size. The maximum in this potential barrier corresponds to the critical radius r^*, where the particle is at equilibrium with the solution monomer as governed by the Gibbs-Thomson equation. The barrier to nucleation can be determined directly by calculating the free energy (ΔG) needed to create a nucleus with size r:

$$\Delta G = \frac{4}{3}\pi r^3 \Delta G_v + 4\pi r^2 \gamma \tag{1.8}$$

where ΔG_v is the change in the Gibbs free energy per unit volume (J/m^3) and is related to the chemical potential energy through $\Delta\mu_v = V_m \Delta G_v$. The first part of 1.8 accounts for the favorable free energy associated to the formation of a defined volume of material, while the second part accounts for the free energy associated with the unfavorable formation of the surface. Figure 1.3 reports the plot of the overall free energy as a function of the particle size. When the particle size increases below the critical radius ($r < r^*$) the free energy of the system increases because the surface component of the Gibbs free energy dominates over the thermodynamically favorable volume component. As the size increases further ($r > r^*$), the volume component begins to make the major contribution to the barrier to nucleation, so that the free energy decreases. The critical radius, corresponding to the barrier maximum, represents the boundary between thermodynamically stable and unstable nanoparticles. Nanoparticles smaller than r^* are unstable, so that they will dissolve, while those that are larger ($r > r^*$) will grow into bigger particles.

The critical radius r^* and the activation energy can be found by setting to zero the first derivative of ΔG :

$$r^* = -\frac{2\gamma}{\Delta G_v} = \frac{2\gamma V_m}{RT \ln S} \tag{1.9}$$

$$\Delta G^* = \frac{4\pi\gamma}{3} r^{*2} \tag{1.10}$$

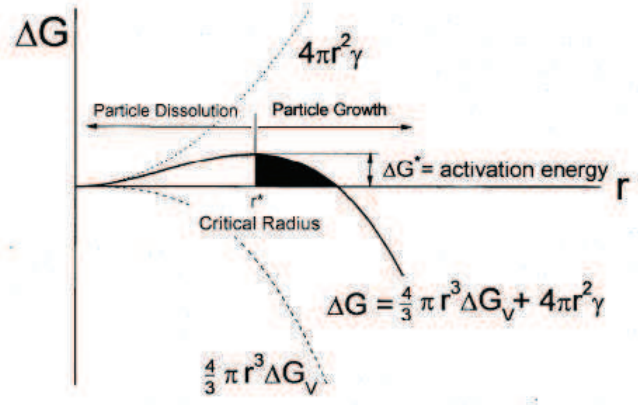

Figure 1.3: A schematic of the Gibbs free energy of nucleation. Particles with a radius $r < r^*$ redissolve, those with $r > r^*$ grow further.

1.2.1.2 Homogenous Nucleation: Kinetic Aspects

The nucleation rate, that is the number of nuclei which form per unit time and volume can be written as:

$$J = K_J \exp\left(-\frac{\Delta G^*}{k_B T}\right) \tag{1.11}$$

where K_J is a factor (weakly dependent on temperature) determined by the frequency of the process and k_B is the Boltzmann constant. Combining equations 1.11 and 1.10:

$$J = K_J \exp\left(-\frac{16\pi V_m^2 \gamma^3}{3N_A^2 k_B^3 T^3 \left(\ln S\right)^2}\right) \tag{1.12}$$

If we observe the plot of J as a function of S (Figure 1.4) we can recognize a metastable zone (under the so-called critical supersaturation) where, even if the solution is supersaturated, nucleation is almost negligible because the

rate J is too low (for low values of γ).

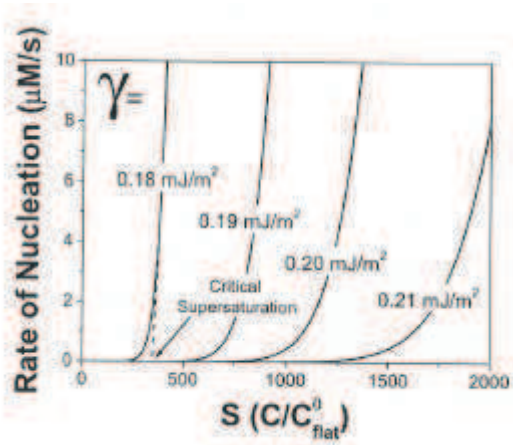

Figure 1.4: The rate of homogenous nucleation given by equation 1.12 for variable γ.

An interplay between thermodynamics and kinetics is always occurring for a given nucleation event. It is important to note that nucleation is always occurring concurrently with growth. As such, the nucleation event coupled with growth acts to rapidly deplete the monomer concentration from the system. The resulting decrease in supersaturation suppress any further nucleation. Growth and Ostwald ripening at this point become the two major mechanisms of evolution for a colloidal ensemble.

Figure 1.5 schematically illustrates the process of nucleation and subsequent growth. When the concentration of the solute increases as a function of time, the nucleation occurs if the supersaturation reaches a certain value above the solubility. After the initial nucleation, the concentration of the solute decreases and the change of Gibbs free energy reduces; there is a moment in which nucleation and growth are inseparable processes. When the concentration decreases below a specific concentration, which corresponds to the critical energy, no more nuclei would form, whereas growth will pro-

ceed until the concentration of growth species has attained the equilibrium concentration or solubility.

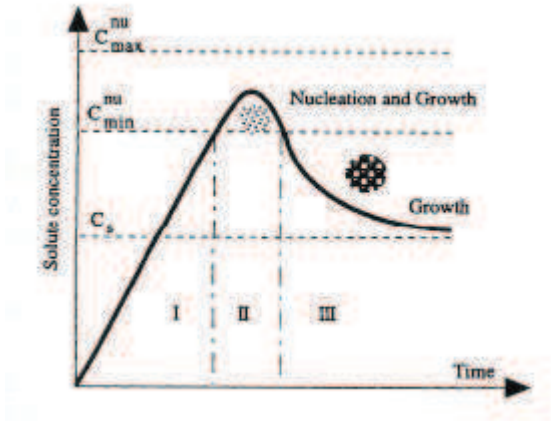

Figure 1.5: Schematic of the process of nucleation and subsequent growth (La Mer's diagram [31]).

1.2.1.3 Mechanism of Growth

For the preparation of nanoparticles with uniform size distribution, it is best if all nuclei are formed at the same time. In this case, all the nuclei are likely to have similar size, since they are formed under the same conditions. In addition all the nuclei will have the same subsequent growth. In practice, to achieve a sharp nucleation, the concentration of the growth species is increased abruptly to a very high supersaturation and then quickly brought below the minimum concentration for nucleation. The size distribution of nanoparticles can be further altered in the subsequent growth process, depending on the kinetics.

A general analysis of the growth process is important to understand nanocrystal synthesis. In general, the surface to volume ratio in smaller

particles is quite high. As a result of the large surface area, it is observed that surface excess energy becomes more important in very small particles. Hence, for a solution that is initially not in thermodynamic equilibrium, a mechanism that allow the formation of larger particles at a cost of the smaller particles reduces the surface energy and hence plays a key role in the growth of nanoparticles.

Coarsening effects, controlled either by mass transport or diffusion, are often termed the Ostwald ripening process. This process is dominated by the surface energy of the particle. The chemical potential of a particle increases with decreasing particle size so the equilibrium solute concentration for a small particle is much higher than for large particles, as described by the Gibbs-Thompson equation 1.7. The resulting concentration gradients lead to transport of the solute from the small particles to the larger particles [32].

1.2.2 Aggregation

Aggregation phenomena play a critical role in the preparation of many colloidal systems, so that explanations are needed for the condition under which colloids are stable, or how particles themselves can be aggregated or flocculated in a targeted manner [12]. There are two main types of colloidal forces: van der Waals interactions and electrical double-layer interactions [33].

Van der Waals Force

The Van der Waals force (F_{disp}) between two identical spherical particles of radius r at separation D ($D <$ 10-100 nm) can be described by the Hamaker equation [34]:

$$F_{disp} \cong \frac{Ar}{12D^6} \tag{1.13}$$

where A is the Hamaker constant, a property of the material and the environment. Since A is positive, the van der Waals interaction is attractive.

Electric Double-Layer Interactions

Electrostatic interactions originate due to the presence of induced charges at particle surfaces. The charge is concentrated at the particle/solvent interface, forming a thin layer of negligible dimension in comparison with the particle size. The surface charge is compensated by a charge of opposite sign distributed throughout the continuous phase in order to fulfill the overall electroneutrality condition. In the case of polar media (aqueous solutions) an electrical double layer is formed (Figure 1.6), which affects most of the dynamic phenomena occurring in colloidal systems, as well as their stability. However no complete theory has yet emerged on this subject. At present, two main paths of thinking about the double layer exist:

- A phenomenological approach based on the local thermodynamic balance (DLVO theory) [36];
- The statistical-thermodynamic approach [37].

The former approach is less strict and, as such, it is applicable to a broad range of situations of practical interest, while the more general statistical-thermodynamic approach produces rather specific results, so that it is mainly applicable for planar geometry.

Without going into the mathematical details it must be pointed out that the presence of the electrical double-layer creates a potential around the particle called zeta-potential, that is directly related to the surface potential, as shown in Figure 1.6.

The stabilization of nanoparticle dispersions against aggregation requires the presence of an energy barrier between the particles that prevents their approach when the van der Waals attraction is large. Two general mechanisms for the stabilization of suspensions can be offered. The first is referred to as electrostatic stabilization and is based on charge separation and formation of electrical double layers in aqueous medium, which determines the repulsion of particles and prevents aggregation; the second is the use of

surfactants or polymers around the particle surface that prevent, by electrostatic or steric interactions, the formation of aggregates [38]. It has been empirically demonstrated that nanoparticle suspensions with zeta-potential absolute values above 30 mV can be considered stable.

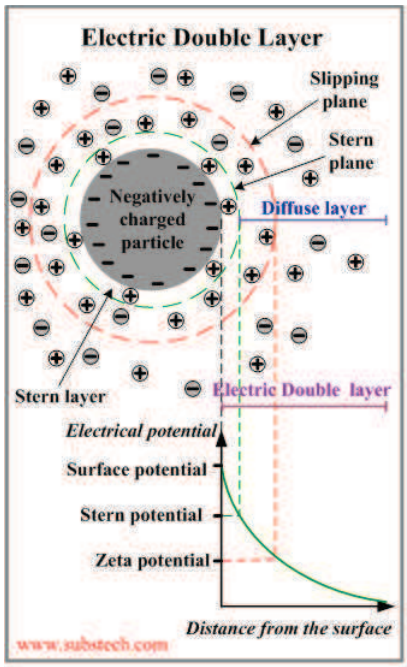

Figure 1.6: Schematic of electrical double layer at the surface of a nanoparticle.

1.3 Characterization Methods

In general it is very hard to follow experimentally the formation of organic nanoparticles from the timepoint when supersaturation is realized, because the particle formation during precipitation occurs on a short time scale, down to millisecond for some systems. In most cases a description of the mechanism of particle formation is still limited to a retrospective derivation from the structure of the particles formed [12]. Anyway, it is possible to follow the formation of nanoparticles by UV-vis spectroscopy and to establish when reprecipitation is complete (Figure 1.2). The formation and the growth of nanoparticles affect the optical properties of the suspension: generally a decrease on absorption maximum (i.e. extinction coefficient) and a shift (often towards the red) of the maximum are observed from the supersaturation time until the end of the process. When no changes are any more detectable on the absorption spectrum of the colloid, the reprecipitation can be considered as come to an end.

Characterization of the as-prepared suspensions is done by using a variety of different techniques, which depend on the properties of interest. Generally, nanoparticle properties are divided in optoelectronic and morphological properties, often related to each other.

1.3.1 Optoelectronic Properties

It was found that the optical and electronic properties of organic nanomaterials are fundamentally different from those of their inorganic counterparts, because the intermolecular interactions in organic materials are basically of weak types, such as hydrogen bonds, π-π stacking, van der Waals contacts and charge transfer (CT) interactions. The resulting properties, such as size-dependent optical properties [39], size-tunable emission, multiple emission [40], tunable/switchable emission [41], aggregation-induced emission [42] are principally studied by UV-vis and fluorescence spectroscopy and fluorescence microscopy in the case of micro-structures. Nonlinear optical properties,

such as two-photon excitation fluorescence (TPEF) and two-photon absorption (TPA), can be studied by TPEF spectroscopy (see Appendix 2) or Z-scan method.

1.3.2 Morphological Properties

There are various techniques for detecting, measuring and characterizing the morphology of nanoparticles. There are methods that give informations on an amount of nanoparticulate material and those that can look at the individual nanoparticle within the sample. Sometimes they are combined to extract more information from one sample.

The common techniques used to characterize the morphology of nanoparticles (size, shape, dispersity) are electron microscopy, such as transmission electron microscopy (TEM) or scanning electron microscopy (SEM), atomic force microscopy (AFM) and dynamic light scattering (DLS), Table 1.1.

1.3.2.1 Microscopy Methods

Transmission Electron Microscopy (TEM) uses an electron beam to interact with a sample to form an image on a photographic plate or specialist camera. The sample must therefore be able to withstand the electron beam and also the high vacuum it is subjected to. The sample preparation is a delicate procedure, as a thin sample on a support grid must be prepared. Furthermore, for organic samples (such as organic nanoparticles), a contrasting agent is required: typically uranyl acetate or ammonium molybdate are used.

Scanning Electron Microscopy also uses a high-energy electron beam but the beam is scanned over the surface and the back scattering of the electrons is looked at. The sample must again be kept under vacuum and it must be electrically conductive at the surface. This can be achieved by sputter coating a non-conductive sample. This requirement can be restrictive and this technique can be time consuming and expensive.

Atomic Force Microscopy is a form of Scanning Probe Microscopy. It

Table 1.1: Morphological characterization techniques for Organic Nanoparticles

Technique	Measures	Sample	Sensitivity
TEM	**Particle size and characterization**	**It must be deposited on a carbon grid and be stable under an electron beam and a high vacuum**	**From 1 nm**
SEM	**Particle size and characterization**	**It must be conductive or sputtered coated**	**From 1 nm**
AFM	**Particle size and characterization**	**It must adhere to a substrate and be rigid and dispersed on the substrate**	**1 nm - 8 μm**
DLS	**Average particle size and size distribution**	**It must be a very diluted suspension**	**10 nm - 10 μm**

uses a mechanical probe to probe the surface of a sample. A cantilever with a nanoscale probe is moved over the surface of a sample and the forces occurring between the probe tip and the sample are measured from the deflection of the cantilever. The deflection moves a laser spot that reflects into an arrangement of photodiodes. This can offer a 3D visualization. Air samples or liquid dispersions can be looked at and AFM is less costly and time consuming than TEM or SEM. However the sample must adhere to a substrate and be rigid and dispersed on it. The roughness of the substrate must be less than the size of the nanoparticles being measured.

1.3.2.2 Dynamic Light Scattering

DLS measures the scattering pattern produced when light is shown through a sample. It combines this with calculations of the diffusion caused by

Brownian Motion in the sample in a relationship described by the Stokes-Einstein equation. This gives an estimation of the average particle size and distribution of particle size through the sample. The sample must be a liquid, a solution or a suspension. It must also be very dilute, otherwise the scattering of light can be unclear. The technique is sensitive to impurities and the viscosity and pH of the sample must be known.

1.4 Experimental

In this section the preparation and characterization of fluorescent organic nanoparticles (FONs) performed in my PhD work are reported. All the nanoparticle suspensions have been obtained through the reprecipitation method, starting from different chromophores (all molecular structures reported in Appendix 1). In particular the experimental studies are focused on a series of families of organic molecules with different properties (described in the next sections):

- Triphenylamine-based derivatives
- Thiophene-based derivatives
- Bodipy-derivatives
- Commercial laser dyes: **Nilered** and **DCM**

The studied systems are surely not exhaustive to describe the variety of organic nanoparticles that could be prepared, but they have been chosen to demonstrate that it is possible to obtain nanoparticles from chemically different organic structures with the specific goal of obtaining fluorescent nanosystems to be exploited for bioimaging or photovoltaic devices. The properties of the obtained nanoparticles (spectroscopic, morphological, stability) depend on the molecular structure of the constituent chromophores and are related to the solid-state properties, but predicting them safely and accurately is not straightforward.

From an empirical point of view, in order to obtain nanoparticles that preserve fluorescence on aqueous suspension, it is necessary to start from a solid-state fluorescent dye, insoluble in water and soluble in organic solvents. However, it must be pointed out that not all organic dyes with the described characteristics yield stable nanosuspensions in water. For example, in some cases (**Nilered** and **DCM**) the nanosuspensions are not stable and precipitate after few minutes or hours, in other cases nanoparticles are

stable during few days and then they aggregate or precipitate. In conclusion it is possible to approximately predict their emitting behavior (if they will be fluorescent or not and the raw color of fluorescence), but it is very hard to predict their stability.

The next sections are divided according to the molecular families. For every family, the most important structural characteristics of the chromophores are introduced and the experimental results about spectroscopy and morphology of the nanoparticles are reported.

1.4.1 Triphenylamine-based derivatives

A series of triphenylamine-based derivatives[1], which belong to the family of conjugated molecules called charge-transfer (CT) or push-pull chromophores, are tested for the preparation of organic nanoparticles (called **T1**, **T2**, **T3** and **T4**, see Figure 1.7).

CT chromophores are constituted by electron-donor (D) and electron acceptor (A) groups, linked by a π-conjugated bridge to form molecules of different symmetry and dimensionality. A dipolar push-pull molecule is composed by a single electron-donor group and a single-electron acceptor group linked together by a π-bridge. A quadrupolar push-pull chromophore has two D (or A) groups linked to an A (or D) group to give linear centrosymmetric structures. In so-called octupolar chromophores a planar structure is formed linking three A (or D) groups to a central D (or A) group, according to a C_3 symmetry axis.

On the basis of this description, **T1** and **T3** are dipolar molecules, while **T2** and **T4** are octupolar chromophores (Figure 1.7). All these triphenylamine-based derivatives have the same electron-donor group, constituted by an amino group; for **T1** and **T2** the electron-acceptor group is an aldehydic group while for **T3** and **T4** a cyano-vinyl or dicyano-vinyl group.

A spectroscopic study of chromophores **T1, T2** and **T3** in different sol-

[1]Synthesized by M. Blanchard-Desce's group.

vents has been achieved by Sissa et al [43].

The experimental results on the obtained nanoparticle suspensions are divided into two groups, according to the molecules and FONs emission: **T1-T2**, that emit in the yellow-orange region and **T3-T4** that emit in the orange-red region.

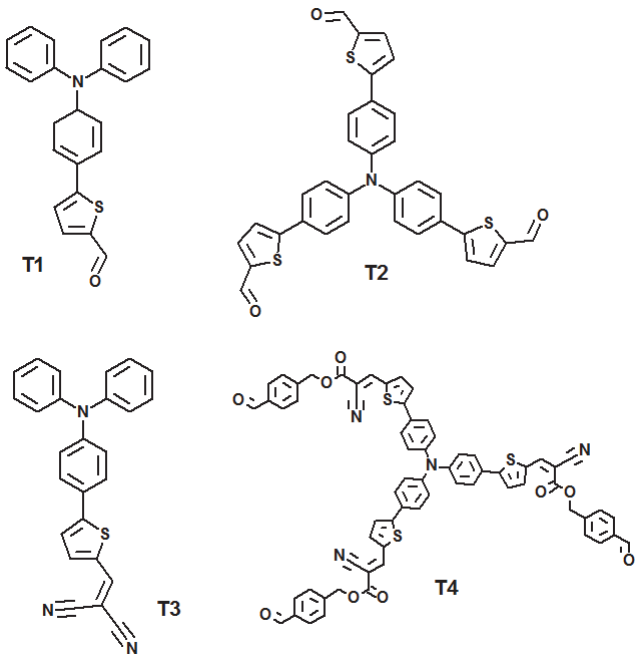

Figure 1.7: Molecular structure of triphenylamine-based chromophores used for the preparation of nanoparticle suspensions.

1.4.1.1 T1 and T2 Nanoparticle Suspensions

Preparation

Nanoparticles of **T1** and **T2** were prepared through the standard reprecipitation process.

Tetrahydrofuran (THF) is chosen as the organic solvent, because the

compounds are well soluble in this medium and high concentrations can be attained. Stock solutions are prepared at a concentration of $1 \times 10^{-3} M$. An aliquot of the organic stock solution is mixed with a known amount of water under vigorous stirring to reach the final nominal dye concentration of 2×10^{-5}M. This corresponds to high dye supersaturation in the medium. To the naked eye, just after mixing, the dye suspensions change color and their fluorescence decreases. The suspension of **T2** FONs remains clear while the suspension of **T1** FONs progressively becomes cloudy. Nanoparticle formation has been monitored through UV-Vis spectroscopy (Figure 1.8): the absorption spectrum of the suspension changes during particle growth. When no further changes are detectable on the absorption spectrum, the nanoparticle formation is considered as accomplished. For **T1** chromophore the reprecipitation process takes place in about 2 hours; the scattering signal increases during time (see the broad spectral feature developing as time elapses, Figure 1.8) because of the growth of nanoparticles and/or the presence of nanoaggregates, thus explaining the cloudiness of the final suspension [17].

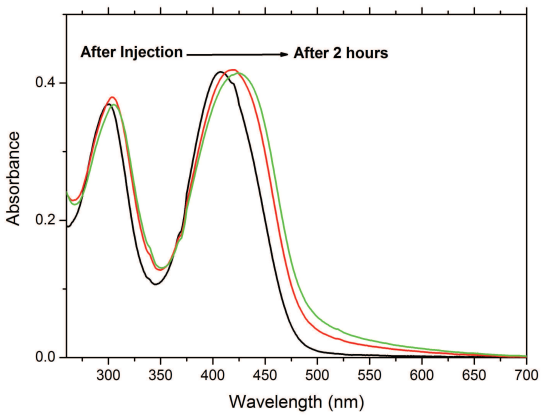

*Figure 1.8: Evolution of the UV-Vis absorption spectrum of **T1***

```
ERROR: undefinedfilename
OFFENDING COMMAND: findfont

STACK:

/
/PRMDPI+
```